Two energetically disparate folding pathways of α-lytic protease share a single transition state

Alan I. Derman and David A. Agard

The Howard Hughes Medical Institute and the Department of Biochemistry and Biophysics, University of California, San Francisco, 513 Parnassus Avenue, Box 0448, San Francisco, California 94143-0448, USA.

The *Lysobacter enzymogenes* α-lytic protease (αLP) is synthesized with a 166 amino acid pro region (Pro) that catalyzes the folding of the 198 amino acid protease into its native conformation. An extraordinary feature of this system is the very high energy barrier (ΔG = 30 kcal mol^{-1}) that effectively prevents αLP from folding in the absence of Pro ($t_{1/2}$ = 1800 years). A pair of mutations has been isolated in the protease that completely suppresses the catalytic defect incurred in Pro by truncation of its last three amino acids. These mutations also accelerate the folding of αLP in the absence of Pro by 400-fold. An energetic analysis of the two folding reactions indicates that the mutations stabilize the transition states of both the catalyzed and uncatalyzed folding reactions by 3 kcal mol^{-1}. This finding points to a single transition state for these two distinct and energetically disparate folding pathways, and raises the possibility that all αLP folding pathways share the same transition state.

A number of proteins are synthesized with large pro regions that are critical for the acquisition of the proteins' native states[1,2]. Prominent among these are the many extracellular proteases of eubacteria as well as a number of vacuolar and lysosomal proteases from eukaryotes[3]. Perhaps the most thoroughly studied example is the bacterial extracellular protease α-lytic protease (αLP), whose large amino terminal pro region (Pro) catalyzes its folding to the native state[4,5]. Once folding is complete, αLP cleaves intramolecularly at the Pro-αLP junction, leaving Pro noncovalently bound as a potent inhibitor of αLP activity[6]. Pro is subsequently digested away, and the native αLP released. In the absence of Pro, αLP when diluted out of denaturant folds rapidly into a stable folding intermediate (Int) with the properties of a molten globule[7]. Int folds spontaneously to the native state at a rate of only 1.2×10^{-11} s^{-1}, which by the application of transition state theory corresponds to an energy barrier of 30 kcal mol^{-1} (ref. 8). Pro accelerates folding by a factor of nearly 10^{10}, to the order of seconds to minutes[9]. This catalysis corresponds to a transition state stabilization of 18 kcal mol^{-1}.

Pro facilitates formation of the native state of αLP both by stabilizing the folding transition state and by forming an inhibitory complex with the native αLP that is more thermodynamically stable than the Int•Pro complex[8]. The folding of αLP in the presence of Pro is thereby driven by thermodynamics, but the maintenance of its native conformation in the absence of Pro is not; the native αLP is at least 3 kcal mol^{-1} less stable than either Int or the denatured protein[8]. αLP is nevertheless trapped in its metastable native state upon digestion of Pro by the large barrier to its unfolding (ΔG = 26 kcal mol^{-1}; $t_{1/2}$ = 1.2 years). The αLP folding reaction illustrates the importance of energy barriers as defining features of any protein folding reaction, both for elucidating the general principles of kinetically controlled reactions such as this, and also, more broadly, for illuminating conventional protein folding reactions where thermodynamic constraints dictate structure. Energy barriers set limits to the searchable conformational space and effectively isolate discrete conformations from one another[10–12].

αLP presents two such barriers for study, the transition states for the catalyzed and uncatalyzed folding reactions. We are interested chiefly in understanding the basis for the inordinately high energy barrier of the uncatalyzed folding transition state, but chose first to study catalyzed folding because of its demonstrated amenability to enzymatic and genetic dissection. Studies of catalyzed folding, where Pro is supplied in *trans* as a separate polypeptide, have revealed that C-terminal truncations of Pro are catalytically defective for folding[9]. Sequential elimination of one to four amino acids substantially diminishes the transition state stabilization that the Pro region provides. Although the binding of Pro to Int, as assessed by the K_M for the folding reaction, is only minimally affected, the k_{cat} decreases by about an order of magnitude with each amino acid removed. The k_{cat} for the folding of wild type αLP with Pro lacking its last three amino acids (Pro-3) is 0.0025 min^{-1}, nearly 1000-fold down from that of the folding with wild-type Pro (Table 1). We therefore sought suppressor mutations in αLP that would offset the catalytic defect of Pro-3. Colonies of *Escherichia coli* transformed with a plasmid containing a hydroxylamine-mutagenized αLP gene expressed bicistronically with Pro-3 were screened for protease activity. A single mutant was repeatedly isolated from a screen of ~175,000 colonies. The mutant contained two mutations, R102H and G134S (αLP R102H/G134S). Suppression of the catalytic defect caused by Pro-3 required that both mutations be present in the protease.

The rate of folding of αLP R102H/G134S catalyzed by Pro-3 was determined with the trypsin-based folding kinetics assay developed for the characterization of wild type αLP. At a con-

Table 1 Catalytic and Michaelis constants[1]

Catalyzed folding	Int•Pro (%)	k'_{cat} (min^{-1})	k_{cat} (min^{-1})	K_M (μM)	$\Delta\Delta G_{Int^{\ddagger}\bullet Pro}$ (kcal mol^{-1})[2]
WT αLP with wt Pro region	85%	0.092 ± 0.00069	1.9 ± 0.17	24 ± 6.1	NA
WT αLP with Pro-3	100%	NA	0.0025 ± 0.00011	4.2 ± 1.1	+2.6
αLP R102H/G134S with Pro-3	15%	0.018 ± 1.4×10^{-7}	3.8 ± 0.26	43 ± 6.4	-2.7
Uncatalyzed folding			k_F (min^{-1})[3]		
WT αLP	NA	NA	7.8×10^{-10}	NA	NA
αLP R102H/G134S	NA	NA	2.9×10^{-7}	NA	-3.2

[1]Values were derived from catalyzed or uncatalyzed refolding experiments as described in Methods. NA, not applicable. WT, wild type.
[2]ΔΔG values are given as positive values for transition state destabilization and as negative values for transition state stabilization.
[3]The k_F value for wild type αLP was calculated from Sohl *et al.*[8] and from S.S. Jaswal (pers. comm.) as described in Methods.

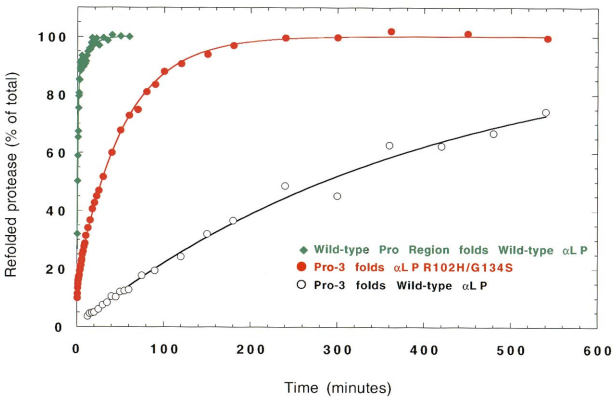

Fig. 1 Catalyzed folding by Pro-3 is accelerated for αLP R102H/G134S. The folding of 5 μM Int was catalyzed by 75 μM Pro region, and the half times for folding calculated from fits of each progress curve. The folding reactions showed biphasic kinetics, with the exception of the folding of wild type αLP with Pro-3, which showed monophasic kinetics (only the early portion of this progress curve is presented). Half time for the folding of wild-type αLP with the wild-type Pro region, 0.58 min; for the folding of αLP R102H/G134S with Pro-3, 28 min; for the folding of wild type αLP with Pro-3, 5 h 4 min.

centration of 75 μM Pro-3, folding proceeded with a half time of 28 minutes, 11 times faster than the folding of wild-type αLP catalyzed by Pro-3 (Fig. 1). The suppression was apparently incomplete because folding was still more than 48 times slower than that of wild type αLP catalyzed by the wild-type Pro region (Fig. 1).

To precisely assess the effects of the suppressor on catalysis, a complete enzymatic profile of the folding reaction was generated. Catalyzed folding of αLP R102H/G134S was carried out with Pro-3 at concentrations ranging from 2 to 125 μM. A fit of the exponential rate constants for the fast phases from the resulting biphasic progress curves gave a value for k_{cat} of 3.8 min^{-1} and a value for K_M of 43 μM (Fig. 2*a*). The k_{cat} is more than three orders of magnitude greater than that for the folding of wild type αLP catalyzed by Pro-3 and it actually exceeds that for the folding of wild type αLP catalyzed by the wild-type Pro region (Table 1).

The apparent discrepancy between the measured k_{cat} and the observed folding rate (Fig. 1) stems from the presence in the folding reaction of a parallel pathway in which the Int•Pro Michaelis complex is isomerized into an alternative conformation (Int•Pro)′ that converts only slowly to product (k'_{cat})[9]. As noted previously, isomerization competes with catalyzed folding and accounts for the slow phase component of the folding progress curves (Fig. 2*b*,*c*)[9]. When Pro-3 catalyzes the folding of αLP R102H/G134S, only 15% of the equilibrium population is Int•Pro, whereas when wild-type Pro catalyzes the folding of wild type αLP, 85% of the equilibrium population is Int•Pro (Table 1). Even though Int•Pro is converted more rapidly to product in the αLP R102H/G134S folding reaction than it is in the wild type folding reaction, there is much less αLP R102H/G134S Int•Pro to start with and so the overall folding is retarded by the slow conversion of the alternative isomer to product.

Although we isolated this mutant to illuminate the mechanism of catalyzed folding, we were of course interested in determining whether the mutations affected uncatalyzed folding as well. The uncatalyzed folding of wild type αLP is so slow that even if it is followed with a highly sensitive thiobenzyl ester substrate for protease activity the time course must be carried out for days in order for the folding rate to be measured[8]. But when Int was prepared from αLP R102H/G134S and assayed with the thiobenzyl ester substrate, we were surprised to find that protease activity could be detected as early as 45 min (Fig. 3). The activity increased linearly over the next few hours and then began to level off as the accumulated protease digested the remaining Int. As expected, no activity was detected in the control wild type αLP preparation. From a linear fit of the data, the rate for the uncatalyzed folding of αLP R102H/G134S was calculated to be 2.9×10^{-7} min^{-1}, a 370-fold acceleration over that of the wild-type protease (Table 1).

This rate enhancement in uncatalyzed folding corresponds to a reduction of 3.2 kcal mol^{-1} in the height of the rate-limiting tran-

a

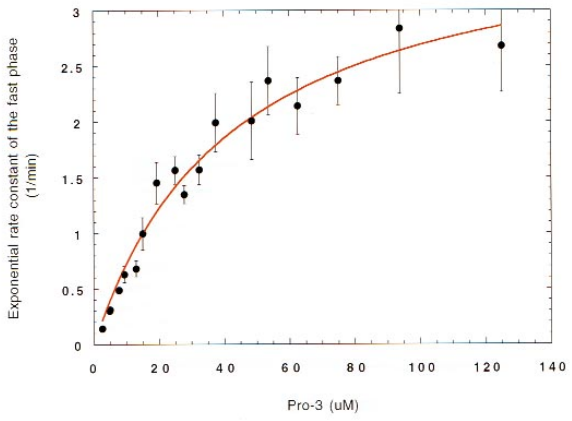

b

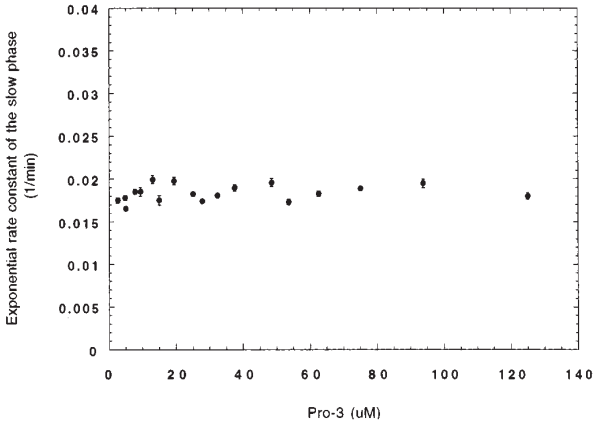

c

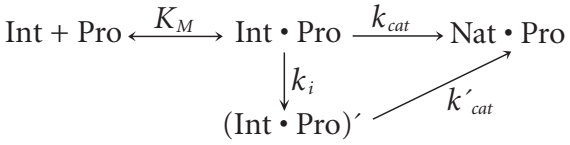

Fig. 2 αLP R102H/G134S suppresses completely the folding defect in Pro-3. ***a***, Catalytic and Michaelis constants for the catalyzed folding of αLP R102H/G134S by Pro-3 were determined from a Michaelis-Menten plot of the faster phase exponential rate constants from individual folding experiments (see Methods). k_{cat} = 3.8 ± 0.26 min^{-1}; K_M = 43 ± 6.4 μM; R = 0.98. ***b***, k'_{cat} for catalyzed folding of αLP R102H/G134S by Pro-3. Plot of the slower phase exponential rate constants from the same experiments (see Methods). k_{cat} = 0.018 ± 1.4 x 10^{-7} min^{-1}. ***c***, Mechanism for the catalyzed folding of αLP. Conversion of the Michaelis complex Int•Pro to product Nat•Pro (k_{cat}) competes with its isomerization to the alternative conformation Int•Pro′ (k_i) which is less productive for folding (k'_{cat})[9].

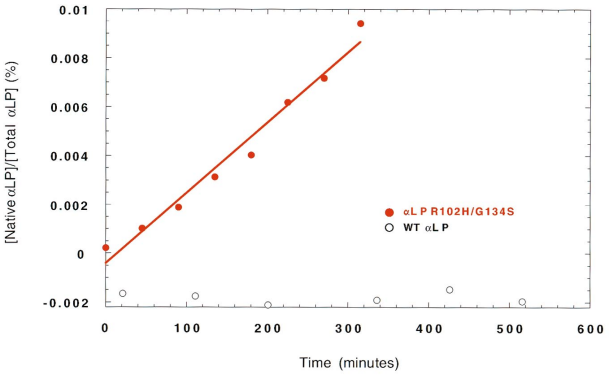

Fig. 3 The rate of uncatalyzed folding of αLP R102H/G134S is greatly enhanced. Intermediate preparations of αLP R102H/G134S (7.1 μM) and of wild type αLP (4.0 μM) were incubated for 9 h, and 820 μl samples of each preparation were withdrawn at 45 min intervals for pepsin treatment and αLP assay. At each time point a smaller quantity of each preparation was also refolded catalytically with 25 μM wild type Pro region. The rate constant of 2.9×10^{-7} min^{-1} (R = 0.98) was calculated from the first 7 h of the experiment because the quantity of refoldable αLP R102H/G134S intermediate began to decline after this point owing to proteolysis by the accumulated protease.

sition state barrier (Table 1). For the catalyzed folding reaction, the reduction in the height of the rate-limiting transition state barrier, calculated from the specificity constant [k_{cat}/K_M] ratio, is 2.7 kcal mol^{-1} (Table 1). Not only do these mutations stabilize the transition states of both the catalyzed and uncatalyzed folding transition states, but they do so to the same extent. It is possible that these two transition states are by chance stabilized equally by these mutations, even though the mutations were isolated solely for their ability to stabilize the transition state for catalyzed folding. The alternative interpretation, which we favor, is that the catalyzed and uncatalyzed folding pathways share the same transition state or at least its critical features, and that there is consequently only one transition state for the mutations to act upon.

This outcome subverted the expectation that mutations in αLP that affect the transition state for catalyzed folding would have limited, if any, effect upon uncatalyzed folding. The landscape for protein folding is commonly modeled as a funnel with a rugged interior, representing an essentially infinite number of possible pathways down to the native state, with each pathway having its own distinct energetic topography[11,12]. This paradigm, which emerged from theoretical studies with lattice models[13,14], has received experimental support. Several proteins whose folding is under conventional thermodynamic control have now been shown to follow multiple pathways to their native conformations[15,16].

It is to be inferred from the ruggedness of the funnel's interior that the transition state for one pathway should not be expected to match or even resemble that of an alternative pathway. The behavior of the chymotrypsin inhibitor from barley (CI2) and the bacteriophage λ repressor is in keeping with this prediction; both proteins show an expansive ensemble of folding transition states[17,18]. But for certain proteins, a surprising amount of conformational homogeneity has been found. Hen egg white lysozyme can fold *via* two pathways, a slow pathway with a discrete intermediate, and a fast pathway with no detectable intermediates; the transition states for the two pathways are energetically identical[19]. A mutation in the α-spectrin SH3 domain that stabilizes its folding transition state and thereby accelerates folding by 20-fold has no effect on its gross conformation, suggesting that the transition state admits of little flexibility, and that there is an obligate set of interactions that must be formed for folding to proceed, regardless of the folding pathway[20].

αLP presents yet another illustration of conformational homogeneity in a folding transition state, and it is an especially clear and dramatic one. Rarely is it possible to isolate and genetically manipulate two entirely distinct and energetically well-characterized folding pathways for a single protein. And in this case, even though 18 kcal mol^{-1} separates the two pathways, it appears that they must pass through the same transition state. We therefore suspect — and more mutational analysis will show whether this is indeed the case — that every route to the native state of αLP must pass through this same transition state.

If the αLP folding transition state ensemble is a single species, it is likely that this occurs because of the costly conformational rearrangements that the transition state species must undergo in order to reach the native protease. If the αLP folding transition state ensemble is a single species, a likely explanation is the costly conformational rearrangements that the intermediate species must undergo to reach the native protease. The inordinately high energy folding barrier implies an extremely cooperative folding reaction. Calorimetric experiments have prompted a substantial role in particular to be ascribed to the entropic penalty associated with folding[8]. Our previous calorimetric experiments have prompted us to ascribe a substantial role in particular to the entropic penalty associated with folding. There may be very few ways or even only one way of meeting the entropic challenge, of concertedly locking the native structure of αLP into place, and thus the conformational heterogeneity of the folding transition state ensemble could be so highly restricted that it is effectively a single species.

It may turn out that what we have found is merely one illustration of a general property of folding landscapes, that conformational homogeneity is actually an intrinsic feature of high energy folding transition states ensembles. If so, then structural information from mutants such as the one described here could prove particularly valuable in leading us to an understanding of the basis for protein folding barriers.

Methods

Isolation of αLP R102H/G134S. Plasmid pP_{A1}phoPro-2+3ph-alp12 contains a bicistronic version of the αLP gene that codes for a variant of the wild type Pro region followed by a wild type αLP gene, each preceded by the segment of the *E. coli phoA* gene that codes for the alkaline phosphatase signal sequence[21]. This plasmid was mutagenized with hydroxylamine for up to 48 h at 70 °C[22], an *Nco*I-*Xba*I fragment containing sequences from the 3′ end of the Pro region to the 3′ end of the αLP gene was cloned into an analogous plasmid containing the gene for Pro-3 in place of the wild type Pro variant, and the resulting ligation mixtures were used to transform strain AD1106 by electroporation. Strain AD1106 is a derivative of strain K10 that carries a chromosomal *lacI*^{Q} mutation derived from strain CAG16188 (ref. 23); strain K10 (obtained as strain DF1000 from D. Fraenkel, Harvard Medical School) was chosen from a survey of several *E. coli* K12 strains on the basis of its superior expression of recombinant αLP. Because of complications arising from recombination events during the screen, subsequent manipulations were carried out in either strain AD1201 or AD1202, which are derivatives of AD1106 that contain the *recA56* mutation[24] from strain CAG12315 or the Δ*recA1398* mutation[25] from strain CAG27020, respectively. All CAG strains were obtained from the laboratory of C. Gross at UCSF. Standard techniques of bacterial genetics were used for strain construction.

Transformants were screened for αLP activity with a nitrocellulose filter-based colony lift assay as described except that αLP expression was induced with 2 or 5 mM IPTG, and the filters were incubated for 10–15 min in a solution of 150 mM NaCl, 5 mM Na-EDTA, 2.5 mg

ml^{-1} gelatin, 0.05% (v/v) NP40, 50 mM Tris-HCl pH 7.5 prior to the colonies being rinsed off[26]. Expression of the wild type αLP in the context of Pro-3 gives essentially no signal in the assay. The αLP R102H/G134S mutation was isolated six times independently after 9 h of treatment with hydroxylamine and three times independently after 12 h of treatment, in all cases as the same two G→A transitions, and in nearly all cases accompanied by one or more silent mutations elsewhere in the sequence. The DNA Facility of the Howard Hughes Medical Institute at UCSF performed all DNA sequencing for the project.

The mutant protease was expressed from a plasmid in which a fragment containing both mutations was subcloned into the monocistronic wild type αLP construct, where the wild type Pro region and αLP R102H/G134S are expressed as a single continuous polypeptide[27]. Expression kinetics and levels were comparable to those for wild type αLP. The protein was purified by S-Sepharose ion exchange chromotography and preparative Mono-S H/R HPLC as described[26], except that the S-Sepharose column was washed with 10 mM glycine, pH 8.4, prior to elution of the protein at pH 9.6. αLP R102H/G134S protease behaved much as the wild type αLP, eluting from the Mono-S column as a sharp peak at about 150 mM sodium acetate.

Pro region purification and αLP denaturation. The Pro regions were purified from inclusion bodies as described[21], except that DNase and $MgCl_2$ were present during the sonication, and the subsequent room temperature incubation was omitted. The wild-type Pro region used has an additional proline at its N-terminus, a cloning artifact that does not affect the behavior of the protein[9]. Protease was denatured as described[9], but denaturation was carried out for 24–36 h. The denatured protease was concentrated to ~1 mM in a centrifugal filter device with a 10 kDa molecular mass cut-off, and the glycine was diluted at least five-fold during the concentration. The integrity of the denatured protease was verified by demonstrating that protease activity recovered upon refolding was consistent with molar absorption measurements at 280 nm.

Catalyzed folding. Catalyzed folding was carried out as described[8], but in 20 mM potassium succinate pH 5.6, and at 0 °C (ice water). Progress curves were generated for at least 10 concentrations of the Pro region, typically ranging from 5 to 125 μM, and these were fit by a three parameter single exponential for the monophasic folding of the wild type αLP with Pro-3, and by a five parameter double exponential for the biphasic folding of the wild type αLP with the wild type Pro region and for the biphasic folding of αLP R102H/G134S with Pro-3. For the last two cases, the percentage of total amplitude present in each phase and also the magnitude of the rate constant for the slower phase were invariant over the entire range of Pro region concentrations, whereas the rate constant for the faster phase increased with increasing Pro region concentration. The amplitudes were fixed at the modal percentage (85% faster phase for the folding of the wild type αLP with the wild type Pro region, 15% faster phase for the folding of αLP R102H/G134S with Pro-3), the progress curves refit by a three parameter double exponential, the magnitudes of the fast phases plotted against Pro region concentration, and the values for K_M and k_{cat} extracted from a fit to the variant of the Michaelis-Menten equation that was derived from the previously demonstrated enzymatic mechanism (Fig. 2*c*)[9]:

$$k_{obs} = \frac{k_{cat}[Pro]}{K_M + [Pro]}$$

The magnitudes of the slow phases were averaged to yield k'_{cat}. For the folding of the wild type aLP with Pro-3, the monophasic exponential rate constants were fit directly to this equation. KaleidaGraph version 3.08d (Synergy Software) was used for higher order analysis of the data and for curve fitting.

Uncatalyzed folding. Uncatalyzed folding was carried out as described[8], but at 0 °C (ice water). Because a 1 ml sample proved adequate for each time point, it was unnecessary to concentrate the pepsin treated material prior to assay. The thiobenzyl ester substrate was used as described, but the concentration of DMSO prior to assay was increased to 5.0% in order to enhance the solubility of the reaction product. The data were corrected for substrate autolysis, and the concentration of native protease determined from a standard curve. The rate constant for the folding of wild type αLP at 0 °C was determined by extrapolation from the data of Sohl *et al*.[8] (25 °C and 4 °C) and from S.S. Jaswal, (pers. comm.) (15 °C).

Acknowledgments

We thank E. Cunningham, J. Sohl, and B. Wilk for assistance in protein preparation, and R. Peters, J. Sohl, and A. Shiau for many helpful discussions. We thank D. Fraenkel and C. Gross for strains of *E. coli* from their laboratory collections, C. Gross for bacteriophage P1 and molecular biology reagents. DNA sequencing was performed at the Howard Hughes Medical Institute DNA Facility. E. Cunningham and S. Jaswal provided critical commentary on the manuscript. This work was supported by the Howard Hughes Medical Institute. A.I.D. was supported by postdoctoral fellowships from the American Cancer Society, the Howard Hughes Medical Institute, and a National Cancer Institute National Institutes of Health Institutional Training Grant administered through the Department of Biochemistry and Biophysics at UCSF.

Correspondence should be addressed to D.A.A. *email: agard@msg.ucsf.edu*

Received 12 November, 1999; accepted 15 March, 2000.

1. Eder, J. & Fersht, A.R. *Molec. Microbiol.* **16**, 609–614 (1995).
2. Baker, D., Shiau, A.K. & Agard, D.A. *Curr. Opin. Cell Biol.* **5**, 966–970 (1993).
3. Shinde, U. & Inouye, M. *Intramolecular chaperones and protein folding* (R.G. Landes, Austin, Texas; 1995).
4. Cunningham, E.L., Jaswal, S.S., Sohl, J.L. & Agard, D.A. *Proc. Natl. Acad. Sci. 0USA* **96**, 11008–11014 (1999).
5. Sohl, J.L. & Agard, D.A. *In Intramolecular chaperones and protein folding* (eds Shinde, U. & Inouye, M.) 61–83 (R.G. Landes, Austin, Texas; 1995).
6. Baker, D., Silen, J.L. & Agard, D.A. *Proteins* **12**, 339–344 (1992).
7. Baker, D., Sohl, J.L. & Agard, D.A. *Nature* **356**, 263–265 (1992).
8. Sohl, J.L., Jaswal, S.S. & Agard, D.A. *Nature* **395**, 817–819 (1998).
9. Peters, R.J. *et al. Biochemistry* **37**, 12058–12067 (1998).
10. Baker, D. & Agard, D.A. *Biochemistry* **33**, 7505–7509 (1994).
11. Chan, H.S. & Dill, K.A. *Proteins* **30**, 2–33 (1998).
12. Dill, K.A. & Chan, H.S. *Nature Struct. Biol.* **4**, 10–19 (1997).
13. Onuchic, J.N., Socci, N.D., Luthey-Schulten, Z. & Wolynes, P.S. *Folding & Design* **1**, 441–450 (1996).
14. Bryngelson, J.D., Onuchic, J.N., Socci, N.D. & Wolynes, P.G. *Proteins* **21**, 167–195 (1995).
15. Goldbeck, R.A., Thomas, Y.G., Chen, E., Esquerra, R.M. & Kliger, D.S. *Proc. Natl. Acad. Sci. USA* **96**, 2782–2787 (1999).
16. Weissman, J.S. *Chemistry & Biology* **2**, 255–260 (1995).
17. Tan, Y.J., Oliveberg, M. & Fersht, A.R. *J. Mol. Biol.* **264**, 377–389 (1996).
18. Burton, R.E., Huang, G.S., Daugherty, M.A., Calderone, T.L. & Oas, T. *Nature Struct. Biol.* **4**, 305–310 (1997).
19. Wildegger, G. & Kiefhaber, T. *J. Mol. Biol.* **270**, 294–304 (1997).
20. Martinez, J.C., Pisabarro, M.T. & Serrano, L. *Nature Struct. Biol.* **5**, 721–729 (1998).
21. Sohl, J.L., Shiau, A.K., Rader, S.D., Wilk, B.J. & Agard, D.A. *Biochemistry* **36**, 3894–3902 (1997).
22. Miller, J.H. *A short course in bacterial genetics* (Cold Spring Harbor Laboratory Press, Plainview, New York; 1992).
23. Brisette, J.L., Russel, M., Weiner, L., & Model. P. *Proc Natl. Acad. Sci. USA* **87**, 862–866 (1990).
24. Lauder, S.D., & Kowalczykowski, S. C. *J. Mol. Biol.* **234**, 72–86 (1993).
25. Bianco, P.R. & Weinstock, G.M. *Nucleic Acids Res.* **24**, 4933–4939 (1996).
26. Mace, J.E. & Agard, D.A. *J. Mol. Biol.* **254**, 720–736 (1995).
27. Mace, J.E., Wilk, B.J. & Agard, D.A. *J. Mol. Biol.* **251**, 116–134 (1995).